TMS motor mapping: Comparing the absolute reliability of digital reconstruction methods to the golden standard

Zeb D. Jonker [a, b, c, *], Rick van der Vliet [a, b], Christopher M. Hauwert [a], Carolin Gaiser [a], Joke H.M. Tulen [d], Jos N. van der Geest [a], Opher Donchin [e, f], Gerard M. Ribbers [b, c], Maarten A. Frens [a, g], Ruud W. Selles [b, c, h]

[a] Department of Neuroscience, Erasmus MC, Rotterdam, the Netherlands
[b] Department of Rehabilitation Medicine, Erasmus MC, Rotterdam, the Netherlands
[c] Rijndam Rehabilitation Center, Rotterdam, the Netherlands
[d] Department of Psychiatry, Erasmus MC, Rotterdam, the Netherlands
[e] Department of Biomedical Engineering, Ben Gurion University of the Negev, Be'er Sheva, Israel
[f] Zlotowski Center for Neuroscience, Ben Gurion University of the Negev, Be'er Sheva, Israel
[g] Erasmus University College, Rotterdam, the Netherlands
[h] Department of Plastic and Reconstructive Surgery, Erasmus MC, Rotterdam, the Netherlands

ARTICLE INFO

ABSTRACT

Background: Changes in transcranial magnetic stimulation motor map parameters can be used to quantify plasticity in the human motor cortex. The golden standard uses a counting analysis of motor evoked potentials (MEPs) acquired with a predefined grid. Recently, digital reconstruction methods have been proposed, allowing MEPs to be acquired with a faster pseudorandom procedure. However, the reliability of these reconstruction methods has never been compared to the golden standard.
Objective: To compare the absolute reliability of the reconstruction methods with the golden standard.
Methods: In 21 healthy subjects, both grid and pseudorandom acquisition were performed twice on the first day and once on the second day. The standard error of measurement was calculated for the counting analysis and the digital reconstructions.
Results: The standard error of measurement was at least equal using digital reconstructions.
Conclusion: Pseudorandom acquisition and digital reconstruction can be used in intervention studies without sacrificing reliability.

Introduction

Transcranial magnetic stimulation (TMS) can be used to measure plasticity in the human primary motor cortex by comparing the location, size and excitability of cortical muscle representations before and after an intervention [1,2]. In the golden standard procedure, data is acquired by measuring electromyography (EMG) while applying multiple stimuli at predefined grid points on the scalp, which is then analyzed by counting the grid points at which more than half of the stimuli produced a motor evoked potential (MEP) [1–4].

Recently, digital analysis methods have been proposed for reconstructing the muscle representation from scattered stimuli, most notably surface fitting [5], cubic spline interpolation [6] and Voronoi tessellation [6]. Cavaleri et al. [7] showed that the surface fitting analysis produces similar results with data acquired in a grid procedure, which takes 15–60 min [4,5], as with data acquired in a pseudorandom walk procedure, which takes less than 5 min [5,7]. Therefore, these reconstruction methods could improve the ability to measure short-term plasticity [5].

To replace the counting analysis, digital reconstruction methods should show at least equal absolute reliability (e.g. standard error of measurement, SEM), as this is a marker of sensitivity to change in an individual or group [8]. However, this analysis has not yet been done. Therefore, the primary goal of this study was to compare the absolute reliability of the motor map parameters (volume, area, center of gravity) of the digital reconstruction methods to the

* Corresponding author. Department of Neuroscience, Erasmus MC, Rotterdam, the Netherlands.
E-mail address: z.jonker@erasmusmc.nl (Z.D. Jonker).

golden standard. The results can be used as reference values for power calculations of future intervention studies.

Material and methods

Twenty-one healthy right-handed subjects were recruited for this study (age: 28 ± 9 years, 12 females). Participants were screened for contraindications using the TMS adult safety questionnaire [9]. The experiment was approved by the Medical Ethical Committee of the Erasmus MC Rotterdam and performed in accordance with the Declaration of Helsinki.

Setup

A Visor2 XT system (ANT Neuro, The Netherlands) was used, consisting of a MagPro X100 stimulator, a MC-B70 coil (Magventure, Denmark), a custom-built amplifier (TMSi, The Netherlands), a Polaris Spectra motion tracking system (NDI, Canada) and Visor 2 software (ANT Neuro, The Netherlands). Electromyography (EMG) signals were recorded from the left first dorsal interosseous (FDI) muscle with silver-silverchloride electrodes in a belly-tendon montage, sampled at 5 KHz and stored for offline analysis.

Experimental protocol

During the whole experiment, participants were seated with their left hand resting pronated on a table. Monophasic TMS pulses with a posterior-anterior current direction were applied over the right hemisphere, with the coil handle pointing 45° from the midsagittal line throughout the protocol. The experimenter received visual feedback of the current coil position as well as previous coil positions color coded with the MEP-amplitudes.

First, the head of the subject was co-registered to a stock MRI scan by defining the nasion, pre-auricular points and at least 100 data points spread out over the scalp. Second, the hotspot, the location with the largest MEPs, was estimated with pseudorandom acquisition using 80 pulses with a 2 s interval [5]. The stimulation intensity was set to 50% of maximum stimulator output (MSO) and increased with 5% MSO if there were no measurable MEPs after 15 pulses. Third, the resting motor threshold (RMT), the lowest stimulator intensity that has $\geq 50\%$ chance to produce a MEP at the hotspot, was determined with the Motor Threshold Assessment Tool (MTAT 2.0) [10]. EMG-responses with a peak-to-peak amplitude ≥ 0.05 mV, between 5 and 45 ms after stimulation, were considered MEPs. Finally, the motor maps were acquired with a stimulation intensity of 110% RMT [4].
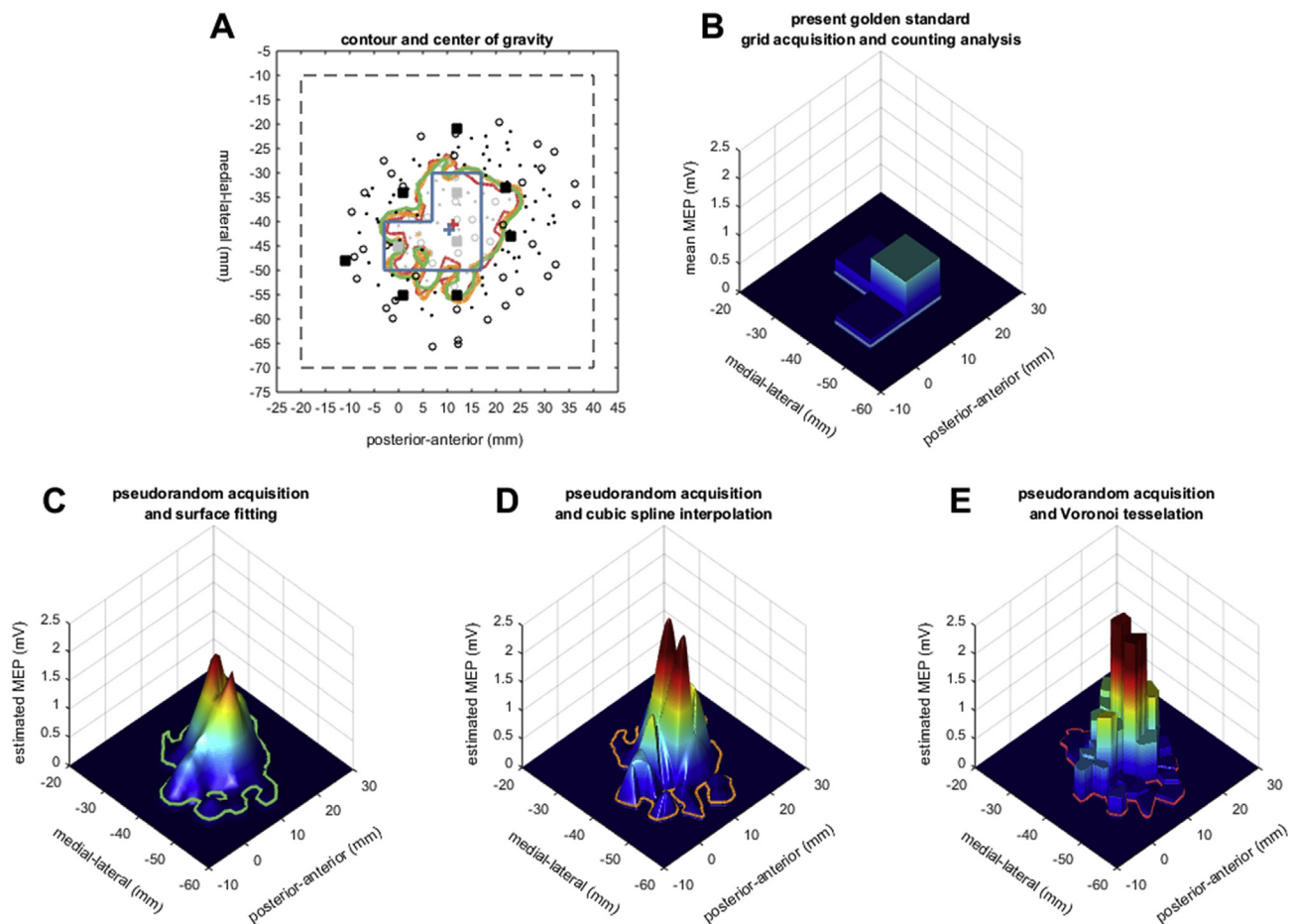
Fig. 1. Methods of pseudorandom data acquisition and digital reconstruction with surface fitting (green), cubic spline interpolation (orange) and Voronoi tessellation (red) compared to the golden standard of grid acquisition and a counting analysis (blue). A: 2D representation of the motor maps. Black and grey markers depict negative and positive stimulation sites: squares depict the grid points of the grid acquisition and circles and points depict the first 50 and remaining 100 stimuli of the pseudorandom acquisition. The estimates of the cog and borders of the motor map are depicted by plus signs and solid lines in the corresponding colors of each method. The dashed square represents a 6-by-6cm predefined region which was used in previous studies with pseudorandom stimulation [5,7,11]. B: 3D representation of the counting analysis after grid acquisition. C–E: 3D representation of the three digital reconstruction methods, after the same pseudorandom acquisition. MEP = motor evoked potential. (For interpretation of the references to color in this figure legend, the reader is referred to the Web version of this article.)

Table 1
Average motor map parameters and standard error of measurement. The averages are denoted with the between subject standard deviation and the standard error of measurement is denoted with the confidence interval. The digital reconstruction methods provide at least equal absolute reliability and produce larger estimates of motor map area and volume.

	Grid acquisition	Pseudorandom acquisition		
	Counting analysis	Surface fitting	Cubic spline interpolation	Voronoi tessellation
Volume log (mV*mm^2)				
Overall Average	4.91 ± 1.14	5.46 ± 1.01	5.45 ± 1.00	5.43 ± 1.00
SEM within	0.53	0.40	0.40	0.39
	[0.41 0.77]	[0.31 0.58]	[0.31 0.58]	[0.30 0.56]
SEM between	0.84	0.47	0.48	0.47
	[0.64 1.21]	[0.36 0.68]	[0.36 0.69]	[0.36 0.68]
Area (mm^2)				
Overall Average	417 ± 165	697 ± 264	654 ± 255	574 ± 236
SEM within	144	107	105	90
	[110 208]	[82 155]	[80 151]	[69 130]
SEM between	177	151	145	120
	[135 256]	[116 218]	[111 209]	[91 173]
xcog (mm)				
Overall Average	17.2 ± 6.9	17.7 ± 6.3	17.8 ± 6.2	17.8 ± 6.2
SEM within	2.0	1.4	1.4	1.4
	[1.6 3.0]	[1.1 2.0]	[1.1 2.0]	[1.1 2.0]
SEM between	3.4	2.1	2.2	2.0
	[2.6 4.9]	[1.6 3.1]	[1.7 3.2]	[1.5 2.9]
ycog (mm)				
Overall Average	-40.3 ± 4.1	-39.3 ± 4.2	-39.3 ± 4.2	-39.3 ± 4.1
SEM within	2.3	1.4	1.4	1.3
	[1.7 3.3]	[1.1 2.0]	[1.1 2.1]	[1.0 1.9]
SEM between	4.2	2.8	2.8	2.7
	[3.2 6.1]	[2.1 4.1]	[2.1 4.0]	[2.0 3.9]
RMT (%MSO)				
Overall Average	45 ± 11	–	–	–
SEM between	1.6	–	–	–
	[1.2 2.3]			

Grid acquisition was based on the well-established paradigm by Kleim et al. (2007) [4]. Ten pulses with an interval of 7 s were applied on the points of a 1-by-1cm spaced grid. A point was marked positive when at least half of the stimuli resulted in a MEP. Grid points were stimulated row by row, moving outward from the center, until a positive area was demarcated by negative points (Fig. 1A).

The pseudorandom acquisition was adapted from Van de Ruit et al. [5] and used 150 pulses. An improvement was made by first creating a subject-specific region of interest with 50 pulses, which prevented muscle representations exceeding the borders of a pre-defined region [7,11]. These 50 pulses were applied in 8 straight lines outward from the hotspot until 2 consecutive pulses (6.8 ± 0.8 mm apart) did not elicit a MEP, followed by a clockwise ellipsoid around these lines (Fig. 1A). The experimenter applied the remaining 100 pulses pseudorandomly inside the ellipsoid.

The grid and pseudorandom acquisition were both performed three times in total (measurement 1–3), twice during the first session and once on the consecutive day. Each session started with determining the RMT, as is done in the follow up of intervention studies [2]. Then, the acquisition methods were performed alternatingly, with the two possible orders counterbalanced between subjects.

Data analysis

From each dataset, four parameters were calculated: area, volume and center of gravity in two dimensions. Data analysis was conducted offline with a custom-made MATLAB script (Mathworks, USA).

First, stimuli were excluded if the root mean square of the background EMG, 100-5 ms before stimulation, was more than 2 standard deviations above the average, or the coil position was outside the 99% probability interval.

Second, a plane was fitted through the 3D coordinates (x,y,z) of the first measurement. The z-coordinates were transposed on this plane. The center of the coordinates (x,y,new-z) was used to translate the coordinates to the origin, which were then subsequently rotated around the x, y and z axis [5]. The same plane, translation and rotation-matrix were used for the other two measurements. For each measurement, the error between the z and new-z coordinates was calculated.

Third, after pseudorandom acquisition, grids were reconstructed with three methods: surface fitting, cubic spline interpolation and Voronoi tessellation. For surface fitting the gridfit algorithm was used to create a 1.2-by-1.2 mm spaced grid [5,7]. For cubic spline interpolation and Voronoi tessellation, the griddata algorithm (method set to cubic or nearest) was used to create 0.1-by-0.1 mm spaced grids [6]. Points in these reconstructed grids where the estimated EMG-amplitude was below 0.05 mV, were set to 0. After standard grid acquisition, the counting of MEPs was repeated offline. For positive points the mean EMG-amplitude was calculated and negative points were set to 0.

Finally, the motor map parameters were calculated. Volume was computed as the sum of the positive cell areas multiplied with their corresponding EMG-amplitudes and area as the sum of all positive cell areas. The cog was calculated for the posterior-anterior (xcog) and the medial-lateral direction (ycog) and added to the translation of the plane.
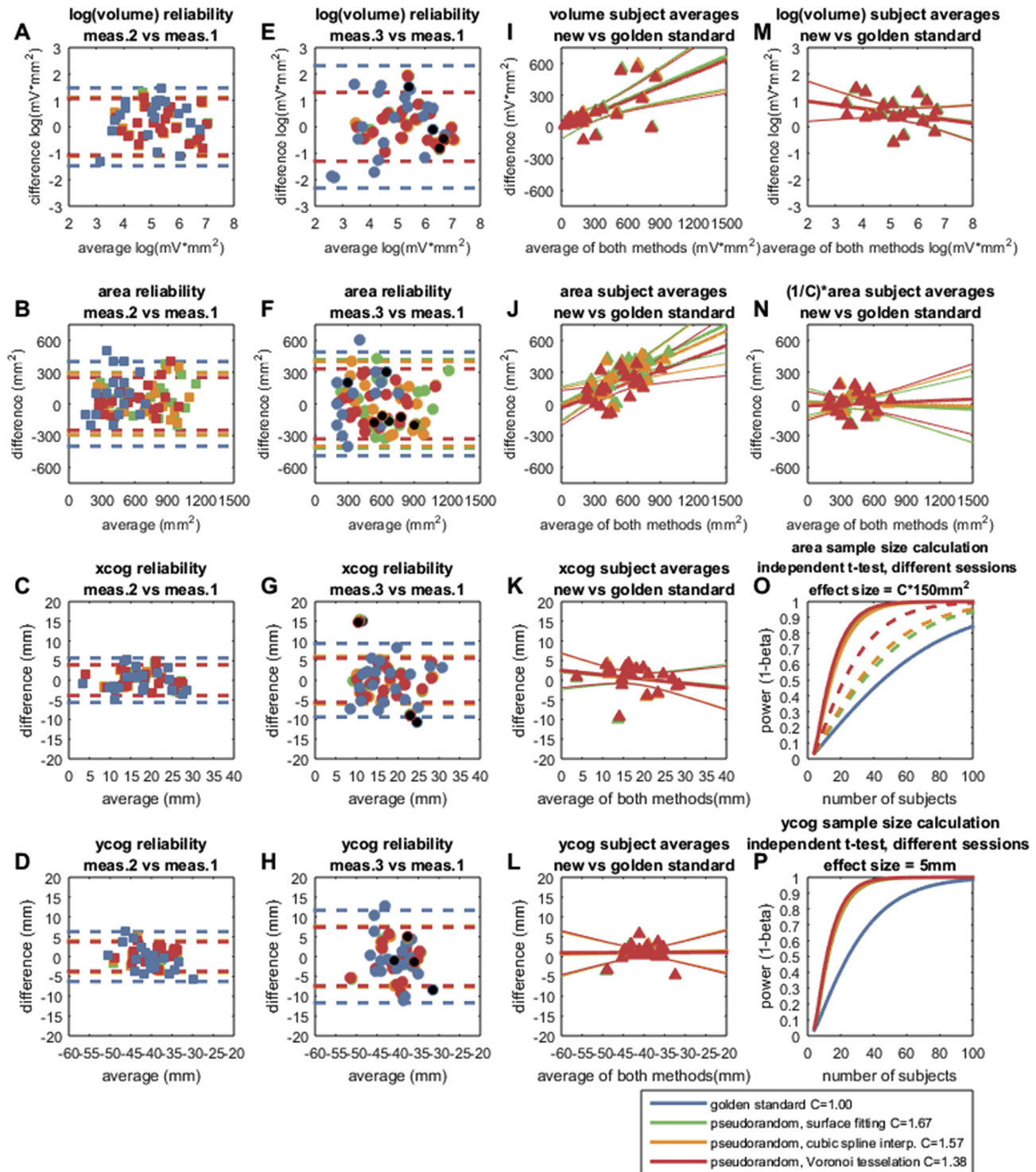
Fig. 2. Results of pseudorandom data acquisition and digital reconstruction with surface fitting (green), cubic spline interpolation (orange) and Voronoi tessellation (red) compared to the golden standard of grid acquisition and a counting analysis (blue). A–H: Bland-Altman plots depicting the within subject differences of each method for measurements acquired in the same session (A–D) or in separate sessions (E–H). Black filled markers depict the two subjects that were removed because of a co-registration error. Dashed lines depict the smallest detectable change, which was smaller for the reconstruction methods, but still large compared to effect sizes found in clinical studies [1,2]. Importantly, the within subject differences did not increase with the averages. This indicates that the methods are equally reliable for small and large muscle representations. I–N: Bland-Altman plots depicting the between method differences of the subject averages. Solid lines depict linear regression lines and their confidence interval. The heteroscedasticity of the volume parameter was successfully removed with a log transformation. The estimations of the area parameter after digital reconstruction were systematically 67% (surface fitting), 57% (cubic spline interpolation) and 38% (Voronoi tessellation) larger compared to the golden standard. O–P: Examples of power calculations (alpha = 0.05) using the absolute reliability of this experiment and the effect sizes from previous clinical studies [1,2], The effect size of area was adjusted for the bias between the methods. Dashed lines depict the power calculation without this adjustment.

Meas. = measurement; C = scaling constant for motor map area; xcog = center of gravity in the posterior anterior direction; ycog = center of gravity in the medial-lateral direction. (For interpretation of the references to color in this figure legend, the reader is referred to the Web version of this article.)

Statistical analysis

First, the subject averages of volume, area, xcog and ycog were calculated for the golden standard and the three digital reconstruction methods. These subject averages were used to inspect the between-method differences with Bland-Altman plots and to compute the overall average of each method.

Second, for each method separately, the within-subject differences between measurement 2 and 1 (same session) and measurement 3 and 1 (separate sessions) were inspected with Bland-Altman plots as well.

Finally, the standard error of measurement of each method was calculated from the standard deviation of these within-subject differences (SEM $= \mathrm{SD}_{\mathrm{diff\_within}}/\sqrt{2}$) as was the smallest detectable change (SDC $= \mathrm{SD}_{\mathrm{diff\_within}}$ * 1.96) [12].

To illustrate the reliability, examples of sample size calculations are provided. Most intervention studies compare the plasticity in a treatment group to a control group. In this scenario, the primary outcome is a change in motor map parameters. Therefore, the $\mathrm{SD}_{\mathrm{diff\_within}}$ of this study is an estimate for the standard deviation of the groups.

The parameter values are denoted as overall average $\pm$ between subject standard deviation and the SEM is denoted with a confidence interval.

Results and discussion

During data analysis, $3.2 \pm 1.9\%$ of the stimuli were excluded. One subject was removed from the within session analysis, because there were no positive sites during the second grid acquisition. Furthermore, two outliers were removed from the between sessions analysis because the xcog (3.3 mm, first session) and the z-error (9.2 mm, measurement 3) indicated a co-registration error. The average z-error was 1.1 ± 0.4 mm, 1.3 ± 0.5 mm and 2.3 ± 0.9 mm for measurement 1, 2 and 3.

The SEM of the reconstruction methods was equal or smaller than the golden standard (Table 1, Fig. 2A–H). Therefore, the present golden standard using 122 ± 44 stimuli in 17 ± 7 min can be replaced by the much faster reconstruction methods using 150 stimuli in 5 min, without sacrificing reliability (Supplementary Figure).

Power calculations indicate the reconstruction methods can reduce the number of subjects needed in intervention studies (Fig. 2O,P). It is important to note that the reconstruction methods increased the area estimates with 67% (surface fitting), 57% (cubic spline) and 38% (Voronoi tessellation) relative to the golden standard (Fig. 2J,N). This bias was circumvented by normalizing the effect sizes to the overall mean of each method.

Regarding individual patients, all motor map parameters showed a considerable SDC and should be interpreted with caution on an individual level (Fig. 2A–H).

Declarations of interest

None.

Appendix A. Supplementary data

Supplementary data to this article can be found online at https://doi.org/10.1016/j.brs.2018.11.005.

References

[1] Liepert J, Miltner WH, Bauder H, Sommer M, Dettmers C, Taub E, et al. Motor cortex plasticity during constraint-induced movement therapy in stroke patients. Neurosci Lett 1998;250:5–8. https://doi.org/10.1016/S0304-3940(98)00386-3.

[2] Sawaki L, Butler AJ, Xiaoyan Leng X, Wassenaar PA, Mohammad YM, Blanton S, et al. Constraint-Induced movement therapy results in increased motor map area in subjects 3 to 9 Months after stroke. Neurorehabilitation Neural Repair 2008;22:505–13. https://doi.org/10.1177/1545968308317531.

[3] Wassermann EM, McShane LM, Hallett M, Cohen LG. Noninvasive mapping of muscle representations in human motor cortex. Electroencephalogr Clin Neurophysiol Evoked Potentials 1992;85:1–8. https://doi.org/10.1016/0168-5597(92)90094-R.

[4] Kleim JA, Kleim ED, Cramer SC. Systematic assessment of training-induced changes in corticospinal output to hand using frameless stereotaxic transcranial magnetic stimulation. Nat Protoc 2007;2:1675–84. https://doi.org/10.1038/nprot.2007.206.

[5] Van De Ruit M, Perenboom MJL, Grey MJ. TMS brain mapping in less than two minutes. Brain Stimul 2015;8:231–9. https://doi.org/10.1016/j.brs.2014.10.020.

[6] Julkunen P. Methods for estimating cortical motor representation size and location in navigated transcranial magnetic stimulation. J Neurosci Methods 2014;232:125–33. https://doi.org/10.1016/j.jneumeth.2014.05.020.

[7] Cavaleri R, Schabrun SM, Chipchase LS. Brain Stimulation the reliability and validity of rapid transcranial magnetic stimulation mapping. Brain Stimul 2018:1–5. https://doi.org/10.1016/j.brs.2018.07.043.

[8] Schambra HM, Ogden RT, Martínez-Hernández IE, Lin X, Chang YB, Rahman A, et al. The reliability of repeated TMS measures in older adults and in patients with subacute and chronic stroke. Front Cell Neurosci 2015;9:1–18. https://doi.org/10.3389/fncel.2015.00335.

[9] Rossi S, Hallett M, Rossini PM, Pascual-Leone A. Screening questionnaire before TMS: an update. Clin Neurophysiol 2011;122:1686. https://doi.org/10.1016/j.clinph.2010.12.037.

[10] Awiszus F, Borckardt J. TMS Motor Threshold Assessment Tool 2.0 Available at: http://www.clinicalresearcher.org/software.html n.d.

[11] van de Ruit M, Grey MJ. The TMS map scales with increased stimulation intensity and muscle activation. Brain Topogr 2016;29:56–66. https://doi.org/10.1007/s10548-015-0447-1.

[12] Bartlett JW, Frost C. Reliability, repeatability and reproducibility: analysis of measurement errors in continuous variables. Ultrasound Obstet Gynecol 2008;31:466–75. https://doi.org/10.1002/uog.5256.